JCTC Journal of Chemical Theory and Computation

ARTICLE

pubs.acs.org/JCTC

Size-Dependent Phase Changes in Water Clusters

Toshihiro Kaneko,[†] Takuma Akimoto,[†] Kenji Yasuoka,[*,†] Ayori Mitsutake,[‡] and Xiao Cheng Zeng[*,§]

[†]Department of Mechanical Engineering and [‡]Department of Physics, Keio University, Yokohama, 223-8522, Japan

[§]Department of Chemistry, University of Nebraska-Lincoln, Lincoln, Nebraska 68588, United States

ABSTRACT: We investigate melting behavior of water clusters $(H_2O)_N$ (N = 7, 8, 11, and 12) by using multicanonical-ensemble molecular dynamics simulations. Our simulations show that the melting behavior of water clusters is highly size dependent. Based on the computed canonical average of the potential energy and heat capacity C_V, we conclude that $(H_2O)_8$ and $(H_2O)_{12}$ exhibit first-order-like phase change, while $(H_2O)_7$ and $(H_2O)_{11}$ exhibit continuous-like phase change. The melting temperature range for $(H_2O)_8$ and $(H_2O)_{12}$ can be defined based on the peak position of $C_V(T)$ and $dC_V(T)/dT$ (where T is the temperature). Moreover, for $(H_2O)_8$ and $(H_2O)_{12}$, the solid- and liquid-like phases separate temporally in the course of simulation. In contrast, no temporal separation of solid- and liquid-like phases is observed for $(H_2O)_7$ and $(H_2O)_{11}$. In light of the notable temporal separation of solid- and liquid-like phases for$(H_2O)_8$ and $(H_2O)_{12}$, an alternative computer approach for estimating the melting temperature range is proposed based on the time-dependent Lindemann parameters. We find that the melting temperature range estimated from both definitions is consistent with each other for $(H_2O)_8$ and $(H_2O)_{12}$ but not for $(H_2O)_7$ and $(H_2O)_{11}$. We also find that the melting behavior of small water clusters can be conveniently assessed if the energy differences of neighbor-sized clusters at zero temperature are known.

1. INTRODUCTION

Freezing of bulk water is a classical example of the first-order phase transition. Even in highly confined systems, e.g., when water is confined to a carbon nanotube or between two graphene sheets with a nanoscale separation, the freezing transition is still the first order but can become continuous under certain conditions due to the confinement effects.[1,2] On the other hand, for finite-size systems, such as molecular or atomic clusters, the melting-like phase change can be dramatically different from their bulk counterparts. The first experimental evidence of size-dependent melting behavior in atomic clusters was reported by Schmidt et al.[3] More recently, Jarrold and co-workers have observed that small gallium and tin clusters melt at temperatures higher than the melting temperature of bulk metals.[4,5] Although the melting behavior of clusters is strongly size dependent, it would be desirable to seek some generic features on their phase-change behavior.

Small water clusters have attracted considerable interest because the underlying intermolecular interactions and hydrogen-bonding dynamics can be more precisely described on the molecular level in these finite-size systems. In turn, the study of the finite-size water clusters provides more accurate models of water, which may lead to improved understanding of bulk water.[6−24]

Unlike bulk matters, it has been shown that different "phases" can coexist in clusters dynamically without showing phase separation.[25,26] Indeed, dynamical coexistence and reversible structural change have already been observed in simulations of $(H_2O)_6$, $(H_2O)_8$, and $(H_2O)_{20}$ water clusters by a number of research groups.[6,15,16,27] Tsai and Jordan[6] perhaps were the first to show a simulation evidence of the solid-to-liquid like transition in $(H_2O)_8$ clusters. Later, Laria et al.[15] demonstrated that the transition between liquid and solid $(H_2O)_8$ did not involve the passage over an energetic barrier. Shin et al.[18] and Frantsuzov et al.[22] have investigated quantum effects on the melting of $(H_2O)_8$ cluster. Both groups have shown that the quantum effects shift the melting temperature toward a lower value, about 8−25 K below the value obtained from the classical simulation for $(H_2O)_8$. On the other hand, for small-sized water clusters with odd number of molecules, such as $(H_2O)_7$, Tharrington and Jordan[16] have shown that they typically do not undergo a well-defined melting transition; in particular, $(H_2O)_7$ may display "glass-like" behavior. Today, it has been well established that the dynamical coexistence in small clusters is due to the existence of many local minima on the potential energy surface, and as such, it can be difficult to exactly compute the heat capcity from conventional molecular dynamics simulation. Since the heat capacity is a very important parameter to characterize phase transition, in this study, we have employed an efficient simulation method, namely, the multicanonical (MUCA)-ensemble method to compute the canonical average of heat capacity. The MUCA-ensemble method was originally developed by Berg and Neuhaus[28,29] and later extented to work with molecular dynamics (MD) simulation methods.[30,31] Compared to conventional MD methods, the MUCA-MD can sample a wider range of potential energy surface without having the system trapped in local minima. In a previous study, we investigated melting behavior of the Lennard-Jones clusters using the MUCA-MD method.[32] Here, based on the MUCA-MD simulations, we show that small water clusters entail much richer melting behaviors than small LJ clusters.

2. MODEL AND SIMULATION METHOD

The TIP4P water model[33] is used in all simulations, and the free-boundary condition is applied in the MD simulations. Initial coordinates for molecules in water clusters are taken from the Cambridge Cluster Database[34] which provides the global minima of the clusters at 0 K. Initial velocities of molecules are set such that the momentum, and the angular momentum of the clusters are zero. To integrate Newton's equations, the velocity Verlet algorithm with SHAKE/RATTLE method is adopted.

Received: July 1, 2011
Published: August 30, 2011

The MD simulations are performed in both the MUCA and conventional canonical ensembles. Nosé−Hoover thermostat is applied to control the temperature of the systems. In the simulations, if the distance between the center of mass of molecules becomes greater than 30 Å, the system is viewed as under evaporation, and the simulation will be restarted with the same initial positions for the molecules but with different initial velocities. We have also examined an alternative criterion for defining a water cluster, namely, if the O−O distance is within 4 Å, the two relevant water molecules are viewed as being in the same cluster. A test simulation confirms that the two cluster criterions are consistent with one another.

For each size of clusters, a number of simulations with different (given) multicanonical weight factors are performed. At the end of simulations, results for cluster of the same size are combined by using the weighted histogram analysis method[35−37] to calculate the density of state $n(E)$, where E is potential energy. The simulations are repeated until $n(E)$ is converged. Once $n(E)$ is known, the canonical average of a physical observable $A(E)$ at given temperature T is given by

$$\langle A\rangle_T = \frac{\sum_E A(E)n(E)\exp(-E/k_BT)}{\sum_E n(E)\exp(-E/k_BT)} \quad (1)$$

Based on eq 1, the average potential energy $\langle E\rangle_T$ can be calculated. To estimate the melting temperature of $(H_2O)_N$ clusters, we calculate the heat capacity at constant volume C_V and the temperature derivative dC_V/dT based on the following equations:

$$C_V = \frac{\langle E^2\rangle_T - \langle E\rangle_T^2}{k_BT^2} + 3Nk_B \quad (2)$$

$$\frac{dC_V}{dT} = \frac{\langle (E-\langle E\rangle_T)^3\rangle_T}{k_B^2T^4} - \frac{2\langle (E-\langle E\rangle_T)^2\rangle_T}{k_BT^3} \quad (3)$$

where $\langle E\rangle_T$, $\langle E^2\rangle_T$, and $\langle E^3\rangle_T$ are computed using eq 1.

3. RESULTS AND DISCUSSION

3.1. Static Properties. The computed canonical average of potential energy E, heat capacity C_V and the temperature derivative dC_V/dT are summarized in Figure 1. Two distinct types of curves can be seen in Figure 1: For $(H_2O)_8$ and $(H_2O)_{12}$, the peaks of C_V can be easily identified at 181.6 and 164.6 K, respectively, in Figure 1b; and the corresponding S-shaped curves of dC_V/dT can be observed in Figure 1c. Similar bahavior of the C_V-T curve has been reported previously by Tharrington and Jordan.[16] For $(H_2O)_7$ and $(H_2O)_{11}$, however, no apparent peaks are seen in the C_V-T curves. Instead, modest peaks in the dC_V/dT curves are observed at 122.5 and 163.6 K, respectively in Figure 1c. There is no clear change of slope in the potential energy curves in Figure 1a. According to the Ehrenfest classification, the first-order phase transition exhibits a discontinuity (like a step function) in the first derivative of the free energy, such as the potential energy, so that the heat capacity curve should exhibit a very sharp peak, like a δ function. The second-order continuous phase transition is continuous in the first derivative of the free or potential energies but exhibits a discontinuity in the second derivative of the free energy, such as the heat capacity. For finite-size cluster systems, the sharp discontinuity is smeared out due to the finite-size effect, resulting in more broad peaks for C_V or dC_V/dT curves.[38] Thus, based on calculation of the canonical averaged E,

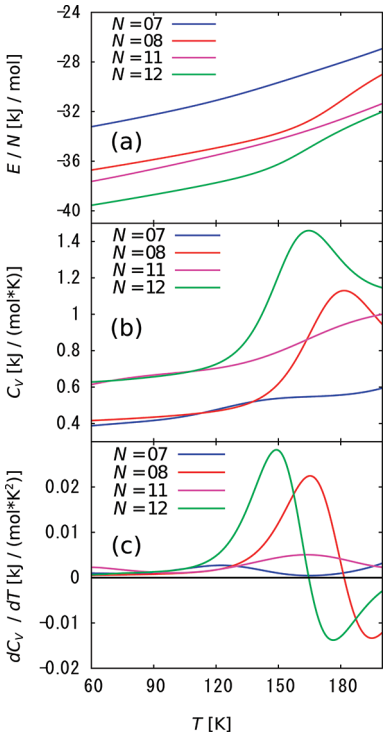

Figure 1. The canonical average of (a) potential energy E, (b) heat capacity C_V, and (c) the temperature derivative dC_V/dT.

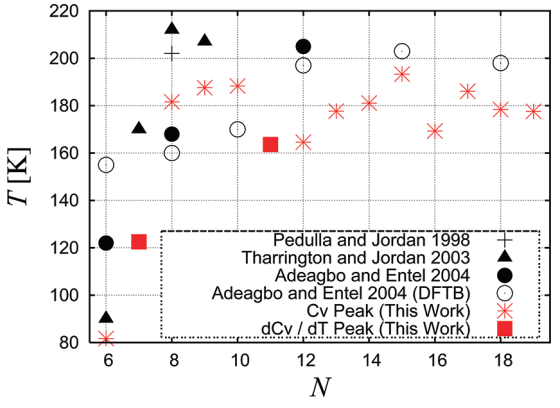

Figure 2. Estimated melting points for each size of small water clusters. For $(H_2O)_7$ and $(H_2O)_{11}$, the melting points are defined by the peak position of dC_V/dT, while for other sizes, the melting points are defined by the position of C_V peak. The water model is TIP4P, except "Adeagbo and Entel, 2004 (density functional-based tight binding)".

C_V and dC_V/dT, we suggest that the first-order-like melting transition occurs for $(H_2O)_8$ and $(H_2O)_{12}$ and continuous-like melting transition occurs for $(H_2O)_7$ and $(H_2O)_{11}$.

Due to the finite-size effects, the melting transition of small clusters does not occur at a single temperature but within a temperature range.[38] Hence, definitions of melting temperature are no longer unique. One possible definition (or C_V based definition) for the melting temperature range associated the first-order-like phase change can be that between the position of the dC_V/dT peak and the position of C_V peak. For clusters exhibiting continuous-like melting transition, such as $(H_2O)_7$ and $(H_2O)_{11}$, one arbitrary C_V-based definition for the melting temparature could be the position of the dC_V/dT peak. In previous

dx.doi.org/10.1021/ct200458m |J. Chem. Theory Comput. 2011, 7, 3083–3087

Table 1. Summary of Estimated Melting Temperature Ranges

N	C_V peak, K	dC_V/dT peak, K	Lindemann parameter, K
7	–	122.5	100–120
8	181.6	165.3	165–180
11	–	163.6	110–130
12	164.6	149.0	150–160

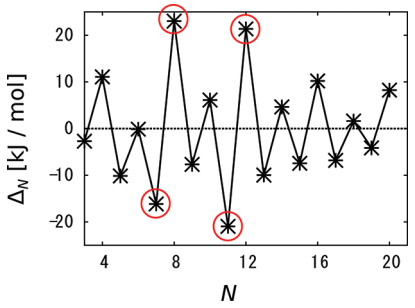

Figure 3. Calculated Δ_N, based on eq 4, for each cluster. It has the maximum values at N = 8 and 12, and the corresponding global-minimum structures are stable. It has the minimum values at N = 7 and 11, and the corresponding global-minimum structures are unstable.

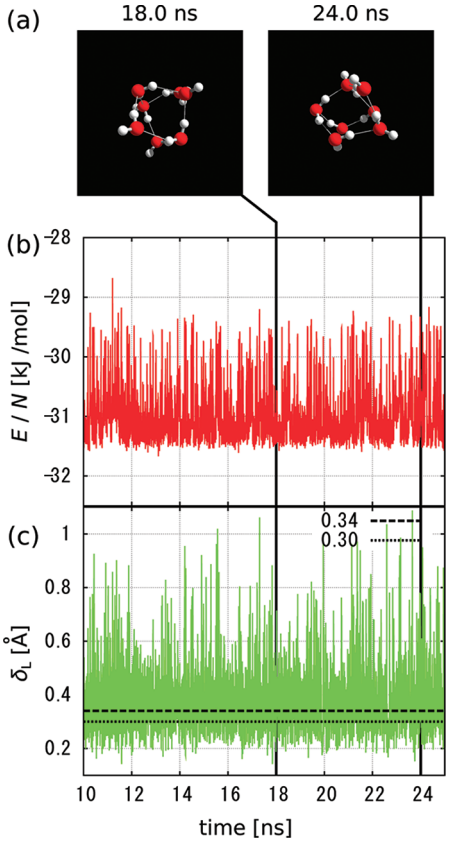

Figure 4. (a) Snapshots of typical structures at two different times, one corresponding to relatively high-energy state and another corresponding to low-energy state (b) potential energy evolution $E(t)$, and (c) the Lindemann parameter $\delta_L(t)$ for $(H_2O)_7$ at 120 K. $E(t)$ and $\delta_L(t)$ are averaged value over every 2.5 ps. No apparent two states (high- and low-energy states) are observed.

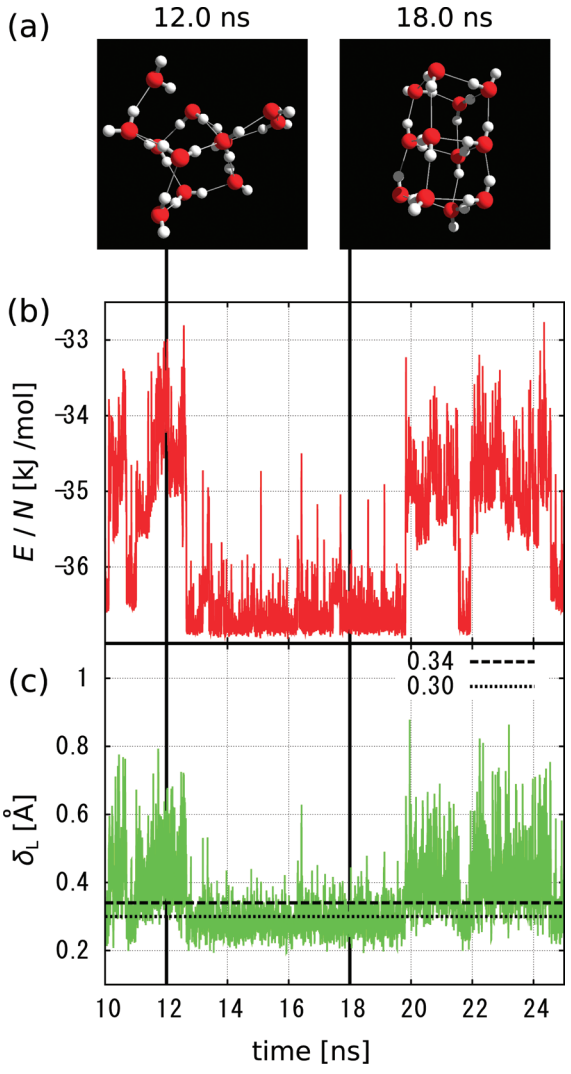

Figure 5. (a) Snapshots of typical structures at two different time, one corresponding to high-energy (liquid-like) state (phase) and another corresponding to low-energy (solid-like) state, (b) potential energy evolution $E(t)$, and (c) the Lindemann parameter $\delta_L(t)$ for $(H_2O)_{12}$ at 150 K. $E(t)$ and $\delta_L(t)$ are averaged value over every 2.5 ps. A temporal intermittency between two states (phases) is clearly seen in (b) and (c). Two horizontal dashed and dotted lines in (c) mark a threshold range for $\delta_{L,th}$ defined to be within 0.30–0.34 Å.

simulations, Pedulla and Jordan calculated C_V of $(H_2O)_6$ and $(H_2O)_8$ using Monte Carlo simulation.[11] Later, Wales and Ohmine[7] revealed the alternation of liquid- and solid-like behavior of TIP4P $(H_2O)_8$ cluster in the course of computer simulation. Their estimated melting temperature was about 190 K. Rodriguez et al.[12] monitored phase transition behavior of water clusters by following the temperature dependence in dipole moments, number of hydrogen bonds, and Lindemann's parameter. They found the melting temperature of TIP4P $(H_2O)_8$ cluster was about 160 K. Tharrington and Jordan also estimated the melting temperature of TIP4P $(H_2O)_{n=6-9}$ based on the position of the C_V peak using the parallel-tempering Monte Carlo method.[16] They found the melting temperature of TIP4P $(H_2O)_8$ cluster was about 215 K, higher than those reported previously. Note that Tharrington and Jordan used a constraining sphere (with radius 4.25 Å) to prevent evaporation. This constraining sphere may inccur some effective

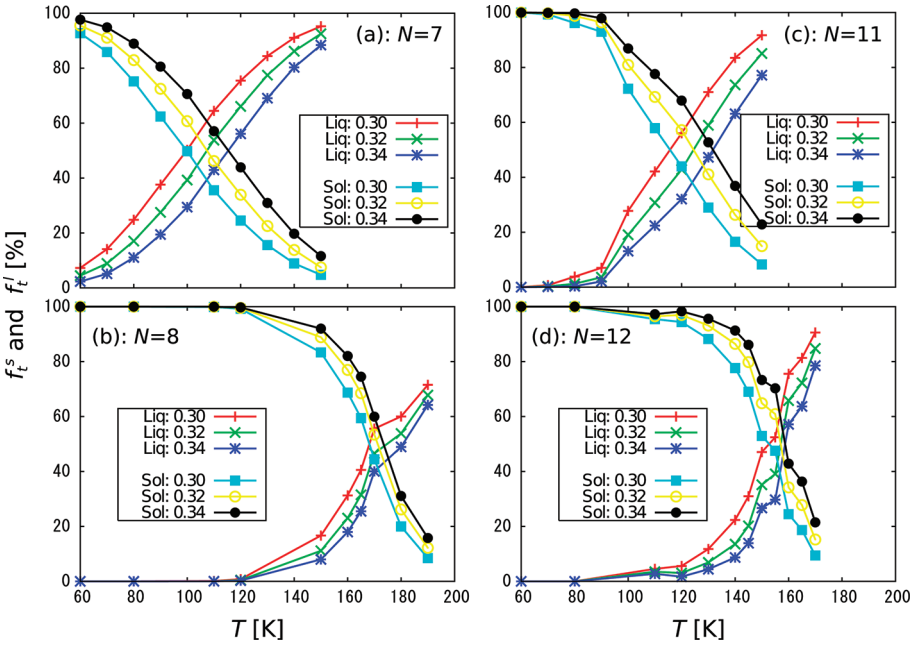

Figure 6. Fraction of time for the system being in the liquid- or solid-like state, determined based the threshold value $\delta_{L,th}$ = 0.30, 0.32, and 0.34, respectively. If $\delta_L(t) < \delta_{L,th}$, then the cluster is viewed to be in the solid-like state, and if $\delta_L(t) > \delta_{L,th}$, then the cluster is viewed to be in the liquid-like state.

"pressure" on the $(H_2O)_8$ cluster, thereby leading to a higher melting temperature for the TIP4P $(H_2O)_8$ cluster. Adeagbo and Entel estimated the melting temperature based on the Lindemann parameter computed from both classical MD and density functional tight-binding (DFTB) simulations.[17] Despite the estimated melting temperature of TIP4P $(H_2O)_8$ cluster ranges from 160 to 215 K among different studies (see Figure 2), the qualitative features of the C_V-T curves from all simulations are the same. The estimated melting temperature ranges or melting temparature are summarized in Table 1.

To gain more insights into the size-dependent phase change, we compute the energy difference Δ_N of neighbor-sized clusters, given by the following equation:

$$\Delta_N = E_{min}(N+1) + E_{min}(N-1) - 2E_{min}(N) \quad (4)$$

where $E_{min}(N)$ is the potential energy of the global minimum at 0 K published previously.[34,39,40] Δ_N corresponds to $d^2E_{min}(N)/dN^2$ or the curvature of $E_{min}(N)$. The results are plotted in Figure 3, where the four clusters considered in this study are marked by red circles. Clearly, Δ_N shows the highest values for N = 8, 12 but the lowest values for N = 7, 11. We suggest that when Δ_N is greater than 20 kJ/mol, like $(H_2O)_8$ and $(H_2O)_{12}$, the corresponding global-minimum structure is very stable, and once the system is trapped in this structure it is difficult to see a phase change for the system. On the other hand, when Δ_N reaches a large negative value (beyond −15), like $(H_2O)_7$ and $(H_2O)_{11}$, the corresponding global-minimum structure is relatively unstable, and the system cannot be trapped in this structure. Hence, the magnitude of Δ_N value offers a guide to the melting behavior (first-order- or continuous-like) for small water clusters. In addition, we have attempted to examine whether the melting temperature of water clusters would converge at certain size. To this end, we have performed several independent simulations to estimate melting temperature of water clusters with size N = 6, 9, 10, 13−19. Interestingly, we find that the melting temperature of $(H_2O)_N$ clusters seems to converge towords 180 K as the size increases (see Figure 2).

3.2. Time-Dependent Properties. To gain additional insights into the size-dependent melting behavior, we further analyze the time-dependent potential energy $E(t)$ and the Lindemann parameter $\delta_L(t)$ of the system in the canonical ensemble. To this end, either 100.05 or 80.05 ns total simulation time is used, in which the initial 0.05 ns is for relaxing the system and is thus excluded from the analysis. The Lindemann parameter $\delta_L(t)$ is given by the equation:

$$\delta_L(t) = \sqrt{\frac{1}{N}\sum_{i=1}^{N}[\langle \mathbf{r}_{O_i}^2(t)\rangle_\tau - \langle \mathbf{r}_{O_i}(t)\rangle_\tau^2]} \quad (5)$$

where N is the number of particles in the cluster, $\mathbf{r}_{O_i}(t)$ is the oxygen position of molecule i, and $\langle\cdots\rangle_\tau$ denotes the time average over a time interval τ (in this study, τ = 2.5 ps). $E(t)$ is also averaged over 2.5 ps time interval.

Results of $(H_2O)_7$ at 120 K are shown in Figure 4. The two snapshots shown in Figure 4a, one corresponding to relatively high-energy state at t = 18.0 ns and another corresponding to low-energy state at t = 24.0 ns, do not show notable difference, suggesting that $(H_2O)_7$ can easily change its conformation structure. Hence, the melting behavior of $(H_2O)_7$ is difficult to discern, which is also reflected by the feature-less behavior of $E(t)$ and $\delta_L(t)$. Similar melting behavior is observed for $(H_2O)_{11}$. Results of $(H_2O)_{12}$ at 150 K are shown in Figure 5. Unlike $(H_2O)_7$, a temporal intermittency between two states is clearly seen, one state is the high-energy (liquid-like) state (phase) and the other is the low-energy (solid-like) state. This means that the cluster exhibits phase change back and forth in the course of simulation, as shown by two typical snapshots in the system, one at t = 12.0 ns and another at t = 18.0 ns (Figure 5a). Note that this temporal separation of low- and high-energy structure in $(H_2O)_{12}$ was also observed in $(H_2O)_{20}$ at 120 K by Nishio and Mikami.[27] Moreover, the time-dependent Lindemann parameter $\delta_L(t)$ shown in Figure 5c suggests that the system stays in the low-energy solid-like state longer than in the high-energy liquid-like state. Based on this observation, we assign a threshold region for $\delta_L(t)$, that is, 0.30−0.34 Å. Note that the

lattice constant of bulk ice is about 3 Å. Hence, 10% of the lattice constant of bulk ice is a sensible parameter to distinguish liquid and solid phases. Using threshold values $\delta_{L,th}$ = 0.30, 0.32, and 0.34, respectively, the fraction of time for the system in the solid- and liquid-like states can be estimated. If $\delta_L(t) < \delta_{L,th}$, then the cluster is viewed as in the solid-like state, and if $\delta_L(t) > \delta_{L,th}$, then the cluster is viewed as in the liquid-like state. The results at various temperatures are summarized in Figure 6. Based on the estimated fraction of time f_t^s and f_t^l for the system being in solid- and liquid-like states, we propose another possible definition for the melting temperature range, that is, the temperature range between the crossing points ($f_t^s = f_t^l = 0.5$) for $\delta_{L,thr}$ = 0.3 and 0.34. Newly estimated melting temparature ranges are given in Table 1. For $(H_2O)_8$ and $(H_2O)_{12}$, we find that the newly estimated melting temperature range is consistent with that based on the position of C_V and dC_V/dT peak. However, for $(H_2O)_7$ and $(H_2O)_{11}$, the newly estimated melting temperature range is notably lower than the melting temperature estimated based on the position of dC_V/dT peak. Hence, the latter may be viewed as an upper limit for the melting temperature of small water clusters that shows the second-order-like phase change.

4. CONCLUSION

We have employed the multicanonical-ensemble molecular dynamics simulation method to investigate melting behavior of small water clusters $(H_2O)_N$ (N = 7, 8, 11, 12). Our simulations confirm that the melting behavior of small water clusters is highly size dependent. In particular,$(H_2O)_8$ and $(H_2O)_{12}$ exhibit first-order-like phase change, while $(H_2O)_7$ and $(H_2O)_{11}$ exhibit continuous-like phase change. Moreover, for $(H_2O)_8$ and $(H_2O)_{12}$, the solid- and liquid-like phases separate temporally in the course of simulation. In contrast, no temporal separation of solid- and liquid-like phases is observed for $(H_2O)_7$ and $(H_2O)_{11}$.

We have proposed two definitions for estimating the melting temperature range associated with the first-order-like phase change: one based on the peak position of $C_V(T)$ and dC_V/dT and another based on the time-dependent Lindemann parameters (in view of notable temporal separation of solid- and liquid-like phases in these clusters). We find that the melting temperature range estimated from both definitions are consistent with each other for $(H_2O)_8$ and $(H_2O)_{12}$. Finally, we suggest that the melting behavior of small water clusters can be conveniently assessed if the energy differences Δ_N of neighbor-sized clusters at zero temperature are known.

AUTHOR INFORMATION

Corresponding Author

*E-mail: yasuoka@mech.keio.ac.jp;xczeng@phase2.unl.edu.

ACKNOWLEDGMENT

T.K. was supported by a Grant in Aid for Japan Society for the Promotion of Science (JSPS) Fellows 23-2003 of the Ministry of Education, Culture, Sports, Science, and Technology (MEXT) in Japan. X.C.Z. was supported by U.S. NSF (grant nos. EPS-1010674 and CBET-1066947) and A.R.L. (grant no. W911NF1020099).

REFERENCES

(1) Koga, K.; Gao, G. T.; Tanaka, H.; Zeng, X. C. *Nature (London)* **2001**, *412*, 802–805.
(2) Han, S.; Choi, M. Y.; Kumar, P.; Stanley, H. E. *Nat. Phys.* **2010**, *6*, 685–689.
(3) Schmidt, M.; Kusche, R.; von Issendorff, B.; Haberland, H. *Nature (London)* **1998**, *393*, 238–240.
(4) Breaux, G. A.; Cao, B.; Jarrold, M. F. *J. Phys. Chem. B* **2005**, *109*, 16575–16578.
(5) Breaux, G. A.; Neal, C. M.; Cao, B.; Jarrold, M. F. *Phys. Rev. B* **2005**, *71*, 073410.
(6) Tsai, C. J.; Jordan, K. D. *J. Chem. Phys.* **1991**, *95*, 3850–3853.
(7) Wales, D. J.; Ohmine, I. *J. Chem. Phys.* **1993**, *98*, 7257–7268.
(8) Gregory, J. K.; Clary, D. C. *J. Phys. Chem.* **1996**, *100*, 18014–18022.
(9) Cruzan, J. D.; Braly, L. B.; Liu, K.; Brown, M. G.; Loeser, J. G.; Saykally, R. J. *Science* **1996**, *271*, 59–62.
(10) Liu, K.; Brown, M. G.; Carter, C.; Saykally, R. J.; Gregory, J. K.; Clary, D. C. *Nature* **1996**, *381*, 501–503.
(11) Pedulla, J. M.; Jordan, K. D. *Chem. Phys.* **1998**, *239*, 593–601.
(12) Rodriguez, J.; Laria, D.; Marceca, E.; Estrin, D. *J. Chem. Phys.* **1999**, *110*, 9039–9047.
(13) Nauta, K.; Miller, R. E. *Science* **2000**, *287*, 293–295.
(14) Keutsch, F. N.; Saykally, R. J. *Proc. Natl. Acad. Sci. U.S.A.* **2001**, *98*, 10533–10540.
(15) Laria, D.; Rodriguez, J.; Dellago, C.; Chandler, D. *J. Phys. Chem. A* **2001**, *105*, 2646–2651.
(16) Tharrington, A. N.; Jordan, K. D. *J. Phys. Chem. A* **2003**, *107*, 7380–7389.
(17) Adeagbo, W. A.; Entel, P. *Phase Transitions* **2004**, *77*, 63–79.
(18) Shin, S.; Son, W.; Jang, S. *J. Mol. Struct. (Theochem)* **2004**, *673*, 109–113.
(19) Aguado, A.; López, J. M. *Phys. Rev. Lett.* **2005**, *94*, 233401.
(20) Bulusu, S.; Yoo, S.; Aprà, E.; Xantheas, S.; Zeng, X. C. *J. Phys. Chem. A* **2006**, *110*, 11781–11784.
(21) Langley, S. F.; Curotto, E.; Freeman, D. L.; Doll, J. D. *J. Chem. Phys.* **2007**, *126*, 084506.
(22) Frantsuzov, P. A.; Mandelshtam, V. A. *J. Chem. Phys.* **2008**, *128*, 094304.
(23) Hock, C.; Schmidt, M.; Kuhnen, R.; Bartels, C.; Ma, L.; Haberland, H.; v.Issendorff, B. *Phys. Rev. Lett.* **2009**, *103*, 073401.
(24) Yoo, S.; Apra, E.; Zeng, X. C.; Xantheas, S. *J. Phys. Chem. Lett.* **2010**, *1*, 3122–3127.
(25) Labastie, P.; Whetten, R. L. *Phys. Rev. Lett.* **1990**, *65*, 1567–1570.
(26) Wales, D. J.; Berry, R. S. *Phys. Rev. Lett.* **1994**, *73*, 2875–2878.
(27) Nishio, K.; Mikami, M. *J. Chem. Phys.* **2009**, *130*, 154302.
(28) Berg, B. A.; Neuhaus, T. *Phys. Lett. B* **1991**, *267*, 249–253.
(29) Berg, B. A.; Neuhaus, T. *Phys. Rev. Lett.* **1992**, *68*, 9–12.
(30) Hansmann, U. H. E.; Okamoto, Y.; Eisenmenger, F. *Chem. Phys. Lett.* **1996**, *259*, 321–330.
(31) Nakajima, N.; Nakamura, H.; Kidera, A. *J. Phys. Chem. B* **1997**, *101*, 817–824.
(32) Kaneko, T.; Yasuoka, K.; Mitsutake, A.; Zeng, X. C. Proceedings of the ASME/JSME 2011 8th Thermal Engineering Joint Conference, Honolulu, Hawaii, March 13−17, 2011; ASME: New York, 2011; AJTEC2011−44457.
(33) Jorgensen, W. L.; Chandrasekhar, J.; Madura, J. D.; Impey, R. W.; Klein, M. L. *J. Chem. Phys.* **1983**, *76*, 926–935.
(34) Wales, D. J.; Doye, J. P. K.; Dullweber, A.; Hodges, M. P.; Naumkin, F. Y.; Calvo, F.; J. Hernández-Rojas Middleton, T. F. *The Cambridge Cluster Database*; Department of Chemistry, Cambridge University: Cambridge, U.K.; http://www-wales.ch.cam.ac.uk/CCD.html.
(35) Ferrenberg, A. M.; Swendsen, R. H. *Phys. Rev. Lett.* **1989**, *63*, 1195–1198.
(36) Kumar, S.; Bouzida, D.; Swedensen, R. H.; Kollman, P. A.; Rosenberg, J. M. *J. Comput. Chem.* **1992**, *13*, 1011–1021.
(37) Mitsutake, A.; Sugita, Y.; Okamoto, Y. *J. Chem. Phys.* **2003**, *118*, 6664–6675.
(38) Berry, R. S.; Beck, T. L.; Davis, H. L.; Jellinek, J. *Adv. Chem. Phys.* **1988**, *70* (2), 75–138.
(39) Wales, D. J.; Hodges, M. P. *Chem. Phys. Lett.* **1998**, *286*, 65–72.
(40) Kazachenko, S.; Thakkar, A. J. *Chem. Phys. Lett.* **2009**, *476*, 120–124.